Int. J. Electrochem. Sci., 10 **(2015)** 10639 - 10650

International Journal of
ELECTROCHEMICAL
SCIENCE
www.electrochemsci.org

Properties of Fluoride-Doped β-PbO_2 Electrodes and their Electrocatalytic Activities in Degradation of Acid Orange II

Qicheng Qiao[1,2,*], *Lizhang Wang*[2,*], *Jian Shi*[3], *Jierong Jin*[1] *and Ya Li*[1]

[1] Deparement of Environment and Resources, Nantong College of Science and Technology. Nantong City, Jiangsu, 226007, P. R. China
[2] School of Environment Science and Spatial Informatics, China University of Mining and Technology. Xuzhou City, Jiangsu, 221116, P. R. China
[3]School of Chemical Engineering and Technology, Nantong University. Nantong City, Jiangsu, 226007, P. R. China
[*]E-mail: qqc1983@126.com, wlzh0731@126.com

Received: 19 September 2015 / *Accepted:* 21 October 2015 / *Published:* 4 November 2015

Fluoride-doped β-PbO_2 anodes were prepared by electrodeposition method to investigate the effect of F^- ion on the performances of the electrodes. The physicochemical properties of the modified β-PbO_2 electrodes were analyzed by spectral methods and electrochemical measurements. The results showed that the surface morphology of the fluoride-doped electrodes held the characteristics of crystal grain of β-PbO_2. The β-PbO_2 electrode doped by 40mM F^- ion had longer service life, higher potentials for the oxygen evolution reaction and more generation of hydroxyl radical(·OH). Furthermore, the acid orange II (AOII) decay on the electrodes were analyzed, and results illustrated that using 40 mM F^- ion was much superior to prepare β-PbO_2 electrode for its higher electrocatalytic activity and mineralization ability.

Keywords: β-PbO_2 electrode; Electrocatalysis; Acid Orange II; Fluoride-doping

1. INTRODUCTION

Electrochemical oxidation treatment, has been described as an environmentally friendly and effective approach for degrading refractory organic pollutants in wastewater because of its strong oxidation performance and easy implementation [1,2]. However, in traditional electrochemical oxidation system, it is necessary to select appropriate electrode materials for effective and economical anodic degradation of pollutants [3]. Therefore, more efficient electrode materials have been discovered by intensive researches including boron-doped diamond (BDD) [4], various dimensionally stable anodes (DSA)(e.g., PbO_2, SnO_2, RuO_2, IrO_2, Pt)[5-10], etc. Up to date, β-PbO_2 has been

extensively studied owing to its easy preparation, low cost, chemical stability, as well as high overpotential for the oxygen reaction [11]. However, pure β-PbO_2 electrode has some drawbacks such as high inner stress, low electrocatalytic activity, and poor stability [12]. Therefore, it is very necessary to enhance the activity and stability of β-PbO_2 electrode by the modification of its film. According to previous researches, the activity and stability of PbO_2 electrode can be increased significantly by addition of small amounts of dopants, such as organic additives and inorganic ions [13-15]. In particular, it has been reported that fluoride doping of the β-PbO_2 electrode can improve its good adhesion to metals, and makes the electrode have long service life, high onset potential for O_2 evolution, and strong catalytic activity for pollutants degradation [16-18]. However, to the best of our knowledge, there are few reports about the influence of different concentration of F^- ion doping on the property and catalytic activity of the modified β-PbO_2 electrodes.

Thus, in this study, we intend to analyze the function of the concentration of F^- ion for the property and catalytic activity of the modified β-PbO_2 electrodes. The effect of the concentration of F^- ion on the microstructure, service life, electrochemical properties and activity for hydroxyl radical (·OH) of the electrodes was investigated employing scanning electron microscopy (SEM), X-ray diffraction (XRD), X-ray photoelectron spectroscopy (XPS), electrochemical techniques and fluorospectrophotometry (FP). In addition, to evaluate the catalytic activity, the degradation efficiency and features of a model pollutant (Acid Orange II, AOII) were also investigated using fluoride-doped electrodes as anodes.

2. EXPERIMENTAL

2.1 Chemicals

A commercial Acid Orange II (4-(2-hydroxynaphthylazo) benzenesulfonic acid sodium salt) purchased from Shanghai Jiaying Chemical Co. Ltd.(China) was used in the present study without further purification. All other reagents were of analytical grade. Before each run, a fresh stock solution of 100mg/L Acid Orange II during all the experimental runs was prepared in deionised water. Sodium sulfate was added as a supporting electrolyte, and the concentration was 3%(w/w).

2.2 Electrode preparation

The Ti plates were pretreated for a good adhesive metal oxide film according to the following procedures. Firstly, Ti plates (2.5cm×2.0cm) were polished by grit sand paper, and then cleansed with water. Secondly, the plates were put into 40 wt% NaOH solution at 333k for 2h, then etched in the boiling solution of 10wt% oxalic acid for 2h to achieve gray surface with uniform roughness. Finally, the plates were washed with deionised water.

After pretreatment, an interlayer of Ti/SnO_2-Sb_2O_3 electrode was prepared on the pretreated Ti plates by thermal decomposition technique using a precursor solution with a nominal composition Sn:Sb=9:1 in mole obtained by dissolving $SnCl_4 \cdot 5H_2O$ and $SbCl_3$ in butanol and hydrochloric acid.

The paint solution was brushed on the pretreated Ti plates, which was dried at 393k for 10min in the oven, and then sintered in the muffle furnace at 773k for 10min. This procedure was repeated ten times. The last baking was kept at 773k for 1h. Finally, the interlayer of Ti/SnO_2-Sb_2O_3 electrode was obtained.

Afterwards, β-PbO_2 films were electrodeposited on the Ti/SnO_2-Sb_2O_3 electrode in 50ml acidic solution which was composed of 0.5M $Pb(NO_3)_2$, 0.1M HNO_3, 0.2M $Cu(NO_3)_2$, and the F^- ion varied to the concentrations of 0, 20, 40 or 80mM through the addition of NaF. The Ti/SnO_2-Sb_2O_3 electrode was used as anode and Ti plate with the same area as cathode. The anode and the cathode with a distance of 1.0cm were vertically inserted in the electrodeposition solution. The time of electrodepositing β-PbO_2 films was 2h with a current density of 20mA/cm^2 at 333k. Finally, the fluoride-doped β-PbO_2 electrodes were thus obtained.

2.3 Electrode characterization

The morphology of fluoride-doped *β*-PbO_2 electrodes was investigated using a scanning electron microscope(SEM, Quanta 250, USA). The structure of the different β-PbO_2 samples was examined by X-ray diffraction (XRD, D8 Advance, GER) with Cu Kα radiation at 40kV and 30mA. Atomic valence state of the β-PbO_2 sample was determined by means of X-ray photoelectron spectroscope (XPS, ESCALAB 250XiX, UK), and an Al Kα monochromatized radiation was employed as X-ray source.

The electrochemical characterization of the fluoride-doped *β*-PbO_2 electrodes was carried out using an electrochemical workstation (CHI 660D, China) in a three-compartment cell, with a standard hydrogen electrode (SCE) as the reference, *β*-PbO_2 electrode as the anode and platinum foil as the cathode. Linear sweep voltammetry (LSV) measurements were taken at an applied scanning rate of 10mV/s between 0 and 2.5V vs. SCE in the electrolyte of 0.5M H_2SO_4 solution.

Accelerated life test was carried out under electrolysis at constant current density of 2A/cm^2 in 1M H_2SO_4 solution controlled at 333k with a thermostat, taking the tested *β*-PbO_2 electrodes as the anode and Ti plate as the cathode. Without special mention, all tests were performed at room temperature.

2.4 Electro-catalytic oxidation activity test

To investigate the electro-catalytic oxidation activity of the electrodes for generating hydroxyl radical (·OH), terephthalic acid solution electrolysis was performed [19]. Terephthalic acid (TA) had a known reaction with ·OH to form fluorescent 2-hydroxyterephthalic acid (HTA). Therefore, TA was used as the probe for ·OH test through the analysis of the fluorescence spectra. When fluoride-doped β-PbO_2 electrodes were employed as anode in 50mL solution composed of 0.5mM TA, 0.25M Na_2SO_4 and 0.5g/L NaOH, electrolyzed solutions were analyzed using spectrofluorimetry at different time. During electrolysis, the sample was measured every 5 min by fluorescence emission spectrum

with a scanning range from 370nm to 520nm.The fluorescence intensity was measured at 425nm with excitation at 315nm by a fluorescence spectrophotometer (RF-5301PC, Japan).

2.5 Electrochemical degradation experiments and analytical methods

An electric power was supplied with regulated DC power supply (APS3500Si, China) for electrolysis. The self-made electrodes (2cm×2cm) were applied as the anode, and Ti plate with the same area was used as cathode. The inter-electrode gap was 1cm. 50mL electrolysis solution, which contained 100mg/L AOII and 3% Na_2SO_4, was stirred with a magnetic stirrer under the current density of 10mA/cm^2. Samples were drawn from the reactor at certain intervals and then analyzed during the experiments.

The UV-visible electronic absorption spectra of Acid Orange II in aqueous solutions was recorded within the wavelength range of 200-700nm using a UV-VIS Spectrophotometers Model (TU-1901, China) with a spectrometric quartz cell(1cm path length). Quantitative analysis of Acid Orange II in aqueous solution was monitored spectrophotometrically by measuring its absorbance at λ_{max}=485nm at different time intervals of electro-oxidation and then computing the corresponding concentration from a constructed calibration curve.

The total organic carbon (TOC) of the initial and electrolysed AOII solution was determined on a TOC apparatus (TOC-L CPH, Japan).

The instantaneous current efficiency (ε_{inst}) for the anodic oxidation of AOII was calculated from the values of TOC using the following relationship [18]:

$$\varepsilon_{\text{inst}} = \frac{2.67[(TOC)_t - (TOC)_{t+\Delta t}]FV}{8I\Delta t} \qquad (1)$$

Where TOC_t and $TOC_{t+\Delta t}$ correspond to the organic carbon concentration(g/L) at a certain time, t (s), and $t+\Delta t$(s); F is the Faraday constant(96,485 C/mol), V (L) is the volume of the electrolyzed solution ,and I(A) is the applied electric current.

3. RESULTS AND DISCUSSION

3.1 Surface morphology and crystal structure

The XRD patterns of the electrodes films doped with different concentrations of F^- ion in Fig.1(a) show that the crystal structure of PbO_2 is pure β-PbO_2 in all the electrodes, which is in good agreement with standard data of the JCPDS card (number:75-2417). It was found that the intensities of β-PbO_2 diffraction peaks were decreased with the F^- ion concentration at 2θ=25.397, 36.224, 52.162, 58.883 and 74.433°, but increased at 2θ=31.982 and 66.866° compared with those of pure PbO_2 anode. Meanwhile, the diffraction peaks were increased with the F^- ion concentration until 80mM at 2θ=62.506°. These phenomena might imply that the F^- ion was successfully introduced into the β-PbO_2 films and the growth of the crystallites was easily attained at certain crystallographic orientations which led to the smaller particle size. In addition, the intensities of the most of the diffraction peaks

decreased sharply and some of them disappeared at 80mM F^- ion, implying that the grain size and the degree of crystallinity of the β-PbO_2 were reduced at high concentrations of F^- ions. XPS patterns, as shown in Fig.1(b), further confirms the existence of F^- ions in the prepared β-PbO_2 electrode at 40mM F^- ion and suggests that some of oxygen sites on surface might be substituted by F^- anions.

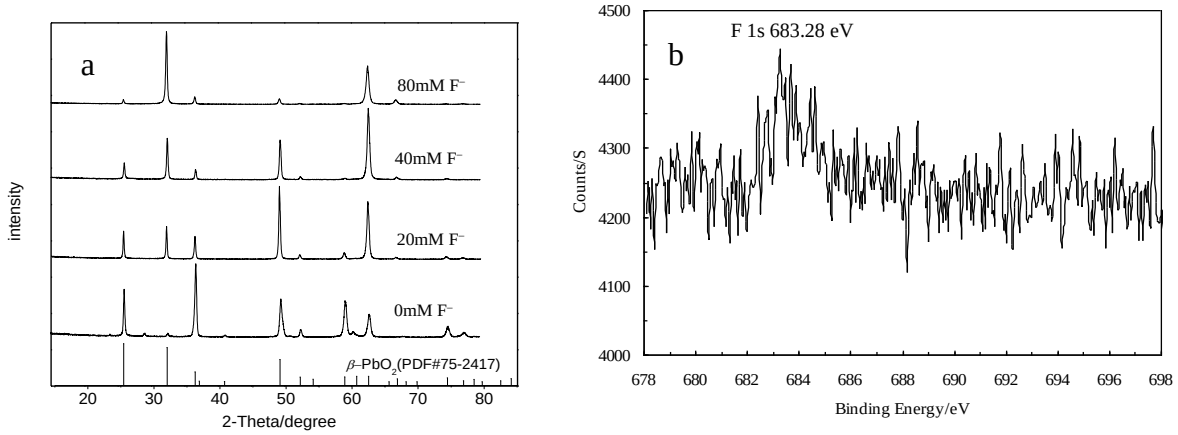

Figure 1. XRD patterns of the β-PbO_2 films electrodeposited using different concentrations of NaF(a) and XPS patterns of F in PbO_2 electrode at 40mM F^- ion (b)

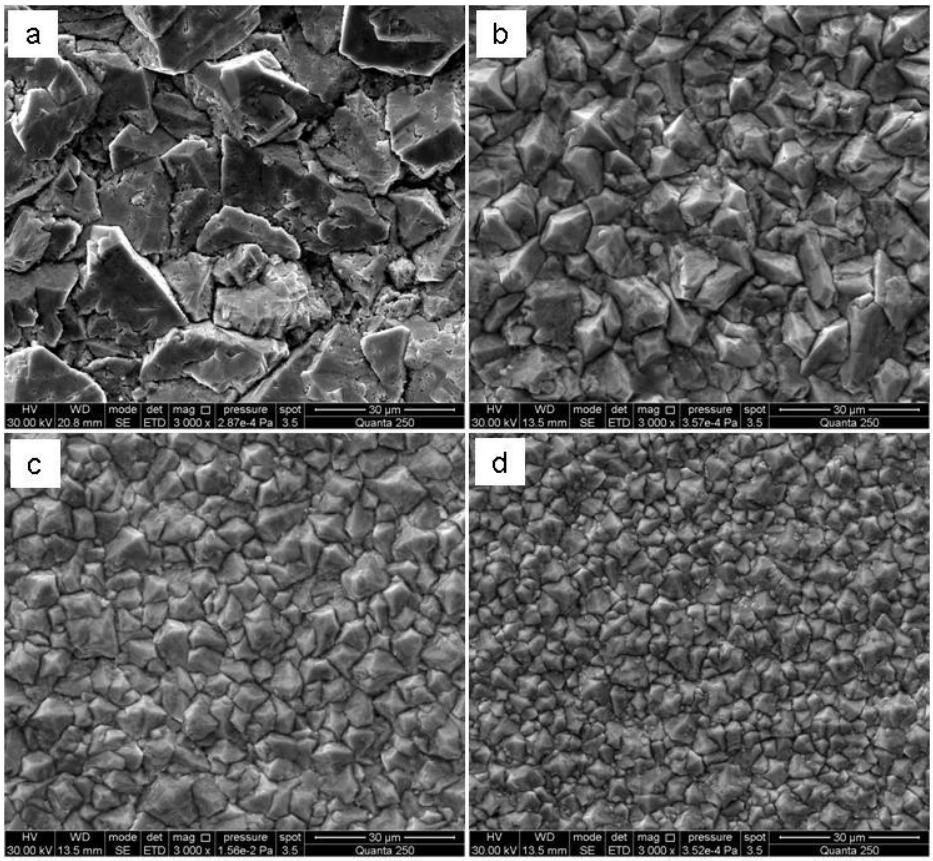

Figure 2. The SEM of β-PbO_2 electrodes under different concentration of NaF (a-0mM F^-, b-20mM F^-, c-40mM F^-, d-80mM F^-)

SEM images of the pure and fluoride-doped PbO_2 electrodes are shown in Fig.2. The morphologies of the electrodes were all presented a typical tetragonal crystallites of the β-phase. In particular, fluoride-doped PbO_2 electrodes showed a more regular morphology and smaller average grain size than the pure electrode, which indicates that F^- ion can be added to the β-PbO_2 phases and hinder the further grain growth. This behavior may be attributed to the substitution of the active oxygen sites by F^- ions in the defect positions of the β-PbO_2 lattice, leading to the formation of smaller crystallites, as the same results of XRD. It is well known that smaller grain size is favorable for the formation of large efficient area, which will improve the absorption of the reactants and catalytic properties of β-PbO_2 electrode [18,20]. Furthermore, due to the high crystallinity and perfect crystal morphology of the film, the electrode could also be helped to reduce the resistance of mass transport, and advance the catalytic activity and stability. However, as could be observed in Fig. 1(a), it seems that the tetragonal morphology was being gradually eliminated at 80mM F^- ion, apparently resulting in an amorphous phase.

3.2 Electrode stability

Service life is an important factor that limits practical application of an electrode [21].Thus, an accelerated electrolysis test was carried out using the pure and fluoride-doped PbO_2 electrodes. Fig. 3 demonstrates the stability of the different PbO_2 electrodes prepared. In accordance with Fig. 3, more protective and adhesive PbO_2 coatings were produced due to the presence of specific amounts of F^- ion in the electrodeposition bath, and it also can be seen that the PbO_2 electrode doped by 40mM F^- ion exhibited the best electrochemical stability. These results indicate that the electrochemical activity and stability of PbO_2 electrode can be improved with appropriate amounts of F^- ion for its preparation. This is in keeping with the statement of Cao et al. [20] that the F^- ion incorporated into the layer of PbO_2 electrode hindered the electrochemical dissolution of the active component and inhibited the formation of insulating layer of oxide between the coating and the substrate.

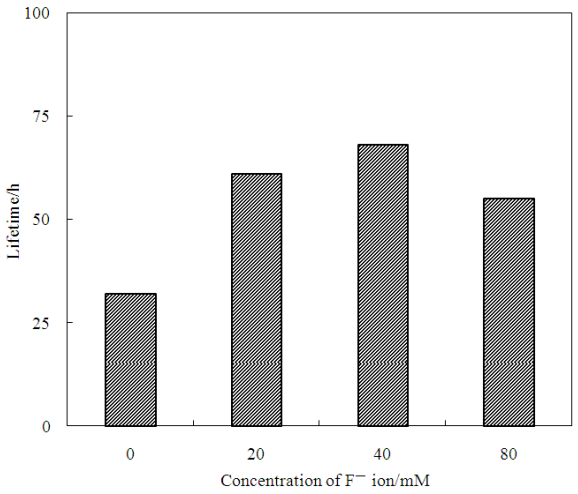

Figure 3. Accelerated life time of β-PbO_2 electrodes electrodeposited using different concentrations of NaF. (The concentration of H_2SO_4: 1M; temperature: 333k; current density: 2A/cm^2).

However, when the F^- ion concentration was increased to 80mM, accelerated lifetime of the PbO_2 electrode decreased quickly. This might be related to the considerable number of defects in the *β*-PbO_2 tetragonal microstructure by large amount of F^- ion, as discussed earlier, which resulted in the amorphous phase of the PbO_2 electrode. Similar results have also been reported by Souza et al.[18].

3.3 Electrochemical measurements

Fig. 4 shows the linear sweep voltammograms for the pure and fluoride-doped PbO_2 electrodes. We can observe that, the modification of *β*-PbO_2 anodes by fluoride leads to considerable increase of the oxygen evolution overpotential (OEP). According to the polarization curves, the OEP value on the *β*-PbO_2 electrode doped by 40mM F^- ion was approximately 1.88V(*vs*.SCE), slightly higher than the 1.75, 1.82 and 1.85V(*vs*.SCE) on the *β*-PbO_2 electrode doped by 0, 20 and 80mM F^- ion, respectively. This result was in agreement with the consequence that the layer of *β*-PbO_2 incorporated of F^- ions led the films to be with lower conductivity [20]. In addition, it is interesting to note that the OEP of the *β*-PbO_2 electrode decreased with the amount of F^- ion at 80mM may due to the amorphous phase. The different values of OEP under different F^- ion concentration reflect the dominating steps of oxygen evolution reaction. When anodic potential enhances, M-OH can be produced by electrochemical reaction between active site (M) and H_2O. Electrode with higher OEP can inhibit the oxygen evolution reaction and facilitate the reaction from M-OH to ·OH [22]. Therefore, *β*-PbO_2 electrode doped by 40mM F^- ion can produce more ·OH with higher current density, which is desired for the electrode's application in the field of electro-catalytic oxidation.

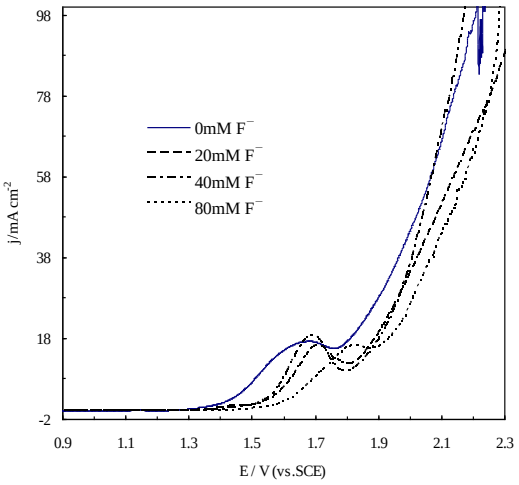

Figure 4. The polarization curves of *β*-PbO_2 electrodes under different concentration of NaF in 0.5M H_2SO_4 solution with a sweep speed of 10mV/s.

3.4 Electro-catalytic oxidation performance

When the four electrodes were employed as anode in electrolysis of terephthalic acid solution, electrolyzed solutions were analyzed using spectrofluorimetry at different time. The fluorescence

emission spectrum of the solution was measured every 5min during in the electrolysis process. As shown in Fig. 5, a gradual increase in the fluorescence intensity of each electrode at 425nm was observed with increasing electrolysis time. It can be found that the fluorescent intensity of PbO_2 electrodes modified by fluoride was higher than that of pure PbO_2 electrode. Meanwhile, fluorescence intensity at 425nm was proportional to the reaction time, indicating the zero-order reaction kinetics was suitable for the oxidation reaction. The rate constants of ·OH generation were 0.067, 0.2982, 0.4369 and 0.2017min^{-1} on the β-PbO_2 electrodes doped by 0, 20, 40 and 80mM F^- ion, respectively, which had the similar trend with the oxygen evolution overpotential. Consequently, it can be found that the β-PbO_2 electrode doped by 40mM F^- ion had the highest fluorescent intensity, suggesting that most ·OH generated on this electrode could be used in the process of decomposing organic matter and raised the current efficiency.

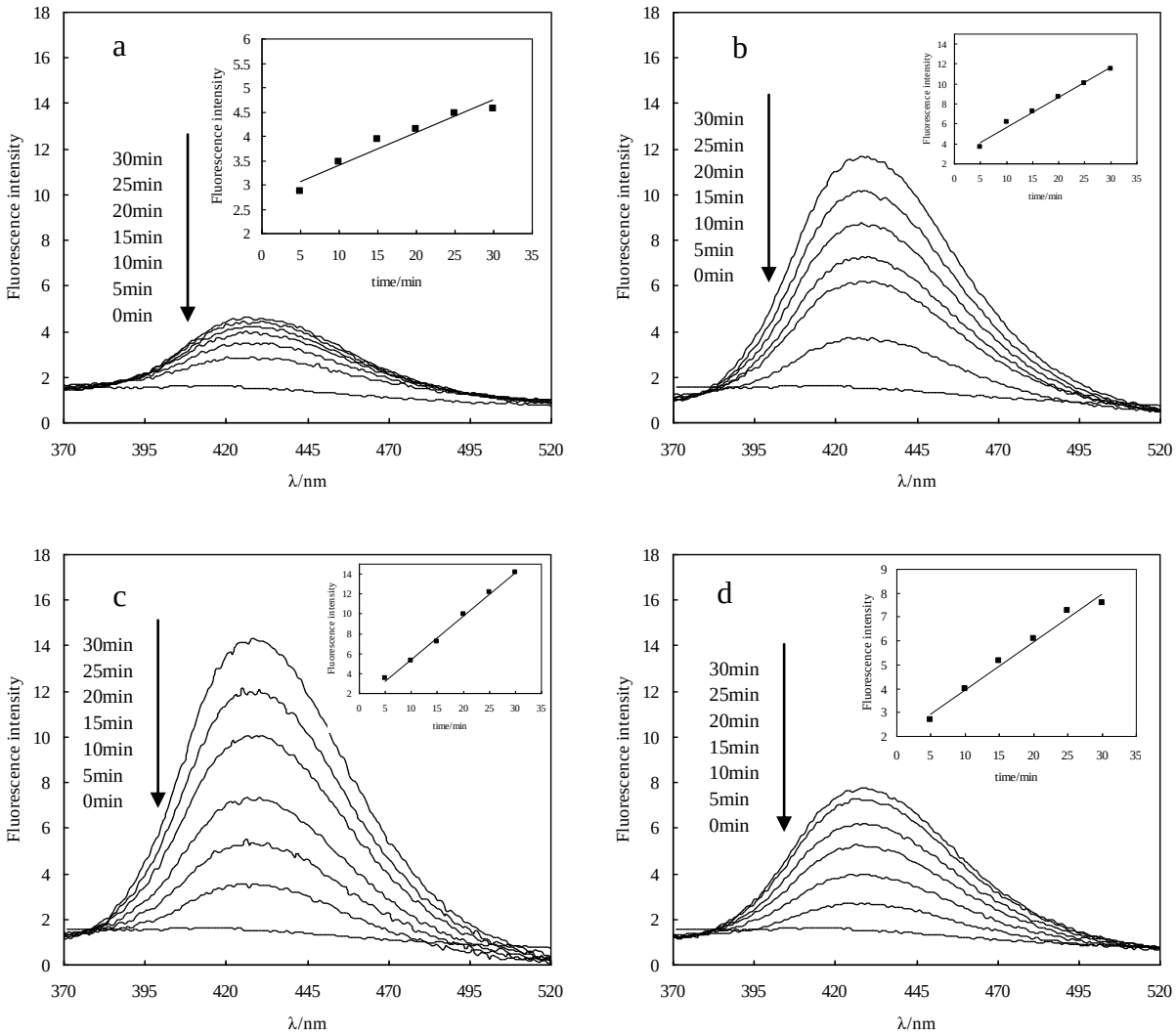

Figure 5. Fluorescence spectra changes observed against reaction time during electro-catalytic oxidation processes in aqueous solution of terephthalic acid on β-PbO_2 electrodes electrodeposited using different concentrations of NaF (a-0mM F^-, b-20mM F^-, c-40mM F^-, d-80mM F^-). (The initial concentration of Terephthalic Acid: 0.5mM; volume:50mL; supporting electrolyte (Na_2SO_4 and NaOH) concentration: 0.25M and 0.5g/L).

The accumulation of ·OH on the surface of β-PbO_2 electrode doped by fluoride might due to the F^- ion occupying channels of the diffusion of the free oxygen atoms, as discussed earlier. However, it seems that considerable number of defects were formed by large amount of F^- ion in the β-PbO_2 tetragonal microstructure, which was not conducive to produce ·OH.

3.5Degradation of Acid Orange II

The electrochemical degradation of AOII was also compared on the four kinds of electrodes, and the variation of AOII removal ratio was presented in Fig.6 (a). It can be seen that AOII was almost all converted on the β-PbO_2 electrode doped by 40mM F^- ion, with the highest removal of 98.7%, after the electrolysis time of 180min. However, at the same time, when the β-PbO_2 electrode doped by 0, 20 and 80mM F^- ion were used as anode, 95.1%, 97.0% and 95.3% AOII removal could be achieved, respectively. The plots of $\ln(C/C_0)$ versus time by utilizing different electrodes were shown in the inset of Fig.6 (a). The linear relationships manifested that the electrochemical oxidation of AOII followed pseudo first-order kinetics. The kinetic rate constants (K), which reflected the reaction rates, were determined from the magnitude of the slopes of the straight lines of each electrode. The result showed that the β-PbO_2 electrode doped by 40mM F^- ion (K =0.0211 h^{-1}) exhibited a higher removal rate of AOII than the β-PbO_2 electrode doped by 0, 20 and 80mM F^- ion (K =0.0178, 0.0207 and 0.0192h^{-1}), respectively. Obviously, above results indicated that the electrochemical oxidation ability of the β-PbO_2 electrode doped by 40mM F^- ion was much higher than those of β-PbO_2 electrodes doped by 0, 20 and 80mM F^- ion.

The results of the electrochemical degradation of AOII could not reflect the mineralization abilities of the pure and fluoride-doped PbO_2 electrodes, so TOC was also used to evaluate the degradation extent of AOII. Fig. 6 (b) demonstrates the TOC removal rate and the resulting instantaneous current efficiency (inset of Fig. 6 (b)) as a function of time. As shown in Fig. 6 (b), there were remarkable differences in TOC removal tendencies. The TOC removal ratios after 180min electrolysis were 47.3%, 53.7%, 57.0% and 46.6% on the β-PbO_2 electrodes doped by 0, 20, 40 and 80mM F^- ion, respectively. As the above discussion, the β-PbO_2 electrode doped by 40mM F^- ion had the greater mineralization rate of AOII due to the greater amount of ·OH generation during water discharge. Meanwhile, it can also be seen that the TOC removal was always less than the AOII abatement, which indicated that AOII oxidation led to the formation of intermediate compounds which might be more recalcitrant. In the inset of Fig. 6 (b), the change of the ε_{inst} with reaction time during the electrochemical treatment was presented. As can be seen from this figure, the ε_{inst} value in the course of electrolysis on the β-PbO_2 electrode doped by 40mM F^- ion was the largest of all. The calculated ε_{inst} according to Eq. (1) was in accordance with the TOC reduction. What's more, the ε_{inst} values were high in the beginning of the electrolysis and gradually decreased because of the removal of AOII and formation of recalcitrant intermediates which were difficult to oxidize.

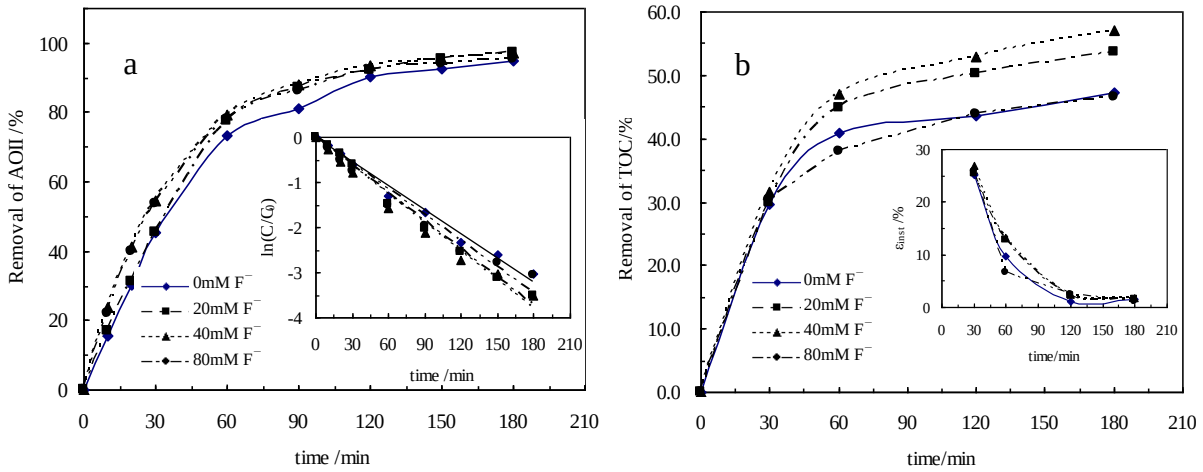

Figure 6. Evolution of AOII degradation efficiency and kinetics of AOII electrochemical degradation (a), TOC degradation efficiency and ε_{inst} (b) with reaction time during the electrolyses on β-PbO_2 electrodes electrodeposited using different concentrations of NaF. (The initial concentration of AOII:100mg/L AOII; volume:50mL; supporting electrolyte (Na_2SO_4) concentration: 3%; current density: 10mA/cm^2).

In order to obtain additional qualitative information about the effect of fluoride-doping in the electro-oxidation processes of AOII on different electrodes, a set of representative UV-vis spectra was presented in this section (Fig.7). As can be seen in Fig.7, the original AOII solution has four characteristic absorption peaks at 229, 255, 310 and 485nm, and one shoulder at 430. The peaks at 229, 255 and 310nm originate from the aromatic rings, and the peak at 485nm and the shoulder at 430nm reflect the conjugated structure formed by azo bond [23]. It is interesting to note that the cyclic intermediates (i.e. benzene ring, naphthalene ring, and their derivatives) can be indicated by variations of the spectra in the ultraviolet region (below 400nm) [23]. In this sense, a comprehensive analysis of Fig.7 was conducted to increase our understanding of the role of different electrodes shown in Fig. 6.

As illustrated in Fig. 7, during electrolysis, the absorption peak of AOII in visible band declined rapidly with increasing electro-oxidation reaction time and until no peak was further observed after about 180min of treatment, it inferred that the cleavage of the N=N and/or C-N bonds of AOII was opened during the electrolysis on all of the electrodes. This also can be confirmed by the color change of degradation solutions. As the reaction proceeded, the solutions changed from orange to pale yellow and then gradually disappeared. On the other hand, the evolution of absorption peaks in UV band was complicated. The absorption at 310 and 229nm were decreased, showing that the aromatic fragment such as naphthalene ring and benzene ring were destroyed. However, the intensity of absorption peak at 255nm increased with time in the first 30min and then decreased, which indicated the complex degradation mechanism involved in the case of electrolyte. In addition, under electrolysis an absorption band around 250nm was appeared, which indicated that some intermediates such as aniline compounds were formed during the degradation of AOII. Comparing with electrode of β-PbO_2 electrode doped by 40mM F^- ion and those of other three kinds of electrodes, the characteristic absorption bands decreased more rapidly and disappeared more thoroughly after about 180min during electrolysis, inferring that 40 mM F^- ion was much superior to be used to prepare β-PbO_2 electrode for

higher electrocatalytic activity and mineralization ability. The results we obtained from UV scan are corresponding with the degradation results.

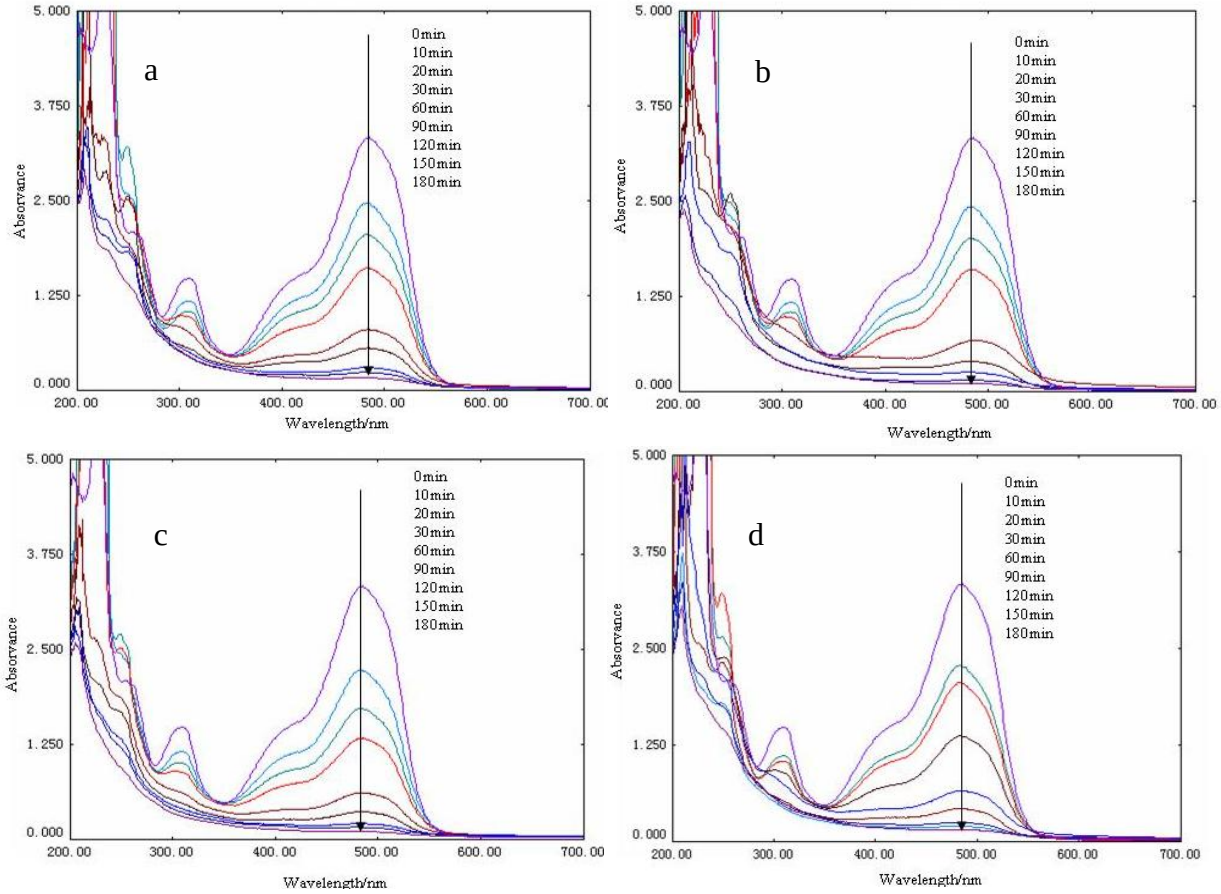

Figure 7. UV-Vis spectral changes of AOII with reaction time during the electrolyses on β-PbO_2 electrodes electrodeposited using different concentrations of NaF (a-0mM F^-, b-20mM F^-, c-40mM F^-, d-80mM F^-). (The initial concentration of AOII:100mg/L AOII;volume:50mL; supporting electrolyte (Na_2SO_4) concentration: 3%; current density: 10mA/cm^2).

4. CONCLUSIONS

In this study, the fluoride-doped β-PbO_2 electrodes prepared by electrodeposition method were investigated. The morphology and component analysis of electrodes showed that the F^- ion could be introduced into the β-PbO_2 film. The crystal structure on the films of the four PbO_2 electrodes was all pure β-PbO_2. The β-phase was growing preferentially at certain crystallographic orientations and smaller crystallites were indicated in the presence of F^- ion. The results of accelerated life tests showed that the service life of the β-PbO_2 electrode doped by 40mM F^- ion was longer than those of other three kinds of electrodes under the same conditions. Specifically, β-PbO_2 electrode doped by 40mM F^- ion also had the desired property of higher potentials for the oxygen evolution reaction, and could generate much more ·OH for decomposing organic matter and raising the current efficiency. The

degradation efficiency and features of AOII were also studied in this study. The results revealed that 40 mM F^- ion was much superior to be used to prepare β-PbO_2 electrode for higher electrocatalytic activity and mineralization ability.

ACKNOWLEDGMENTS
This work was jointly supported by the National Natural Science Foundation of China (Grant No.50908226, No.21177067), Jiangsu Planned Projects for Postdoctoral Research Funds (Grant No.1001022C), Nantong Planned Projects for Applied Research (Grant No.BK2014025) and Natural Science Foundation of Nantong College of Science and Technology for Teachers of Doctor.

References

1. Q. Zhuo, S. Deng, B. Yang, J. Huang, G. Yu, *Environ. Sci. Technol.*, 45 (2011)2973.
2. J. Radienovic, A. Bagastyo, R.A. Rozendal, Y. Mu, J. Keller, K. Rabaey, *Water Res.*, 45(2011)1579.
3. X. Duan, Y. Zhao, W. Liu, L. Chang, X. Li, *J. Taiwan Inst. Chem. E.*, 45 (2014) 2975.
4. S.A. Alves, T.C.R. Ferreira, N.S. Sabatini, A.C.A. Trientini, F.L. Migliorini, M.R. Baldan, *Chemosphere*, 88(2012)155.
5. Q. Dai, Y. Xia, C. Sun, M. Weng, J. Chen, J. Wang, J. Chen, *Chem. Eng. J.*, 245(2014) 359.
6. G.R.P. Malpass, D.W. Miwa, S.A.S. Machado, A.J. Motheo., *J. Hazard. Mater.*, 180(2010) 145.
7. L.H. Tran, P. Drogui, G. Mercier, J.F. Blais, *J. Hazard. Mater.*, 164(2009) 1118.
8. E. Chatzisymeon, S. Fierro, I. Karafyllis, D. Mantzavinos, N. Kalogerakis, A. Katsaou-nis, *Catal. Today*, 151(2010) 185.
9. S. Habibzadeh, D.S. Tim, S. Omanovic, *Int. J. Electrochem. Sci.*, 8(2013)6291.
10. F. Zhang, C. Feng, W. Li, J. Cui, *Int. J. Electrochem. Sci.*, 9(2014)943.
11. D. Deviliers, M.T. Dinh Thi, E. Mahé, Q.L. Xuan, *Electrochim. Acta*, 48(2003) 4301.
12. J. Zhao, C. Zhu, J. Lu, C. Hu, S. Peng, T. Chen, *Electrochim. Acta*, 118(2014) 169.
13. S.P. Tong, C.A. Ma, H. Feng, *Electrochim. Acta*, 53(2008)3002.
14. H. Liu, Y. Liu, C. Zhang, R. Shen, *J. Appl. Electrochem.*, 38(2008) 101.
15. H. Xu, J. Li, W. Yan, W. Chu, *Rare Metal. Mat. Eng.*, 42(2013) 885.
16. J. Cao, H. Zhao, F. Cao, J. Zhang, C. Cao, *Electrochim. Acta*, 54(2009) 2595.
17. R. Amadelli, L. Armelao, A.B. Velichenko, N.V. Nikolenko, D.V. Girenko, S.V. Kovalyov, *Electrochim. Acta*, 45(1999) 713.
18. F. L. Souza, J.M. Aquino, K. Irikura, D.W. Miwa, M.A. Rodrigo, A. J. Motheo, *Chemosphere*, 109(2014) 187.
19. K. Bubacz, E. Kusiak-Nejman, B. Tryba, A.W. Morawski, *J. Photoch. Photobio.A.*, 261(2013) 7.
20. J. Cao, H. Zhao, F. Cao, J. Zhang, *Electrochim. Acta*, 52(2007)7870.
21. W. Yang, W. Yang, X. Lin, *Appl. Surf. Sci.*, 258 (2012)5716.
22. D.D. Johnson, J. Feng, L.L.,Houk, *Electrochim. Acta*, 46(2000) 323.
23. C. Zhang, L. Liu, W. Li, J. Wu, F. Rong, D. Fu, *J. Electroanal. Chem.*, 726(2014) 77.